

Carbon cycle feedbacks during the Oligocene-Miocene transient glaciation

Elaine M. Mawbey and Caroline H. Lear*

School of Earth and Ocean Sciences, Cardiff University, Main Building, Park Place, Cardiff CF10 3AT, UK

ABSTRACT

Ice sheet models suggest that once formed, the large, high-altitude East Antarctic Ice Sheet was relatively self-stabilizing, due to its cold upper surface. The ice sheet hysteresis problem results from an inability to reconcile this expectation with geological evidence for episodes of ice sheet retreat. A classic example of this problem is manifested in benthic foraminiferal oxygen isotope records across the Oligocene-Miocene boundary (ca. 23 Ma), which display a transient $\sim 1\%$ excursion to higher values. The inferred increase and subsequent decrease in ice volume has been linked to advance and retreat of the Antarctic ice sheet across the continental shelf. However, oxygen isotope records alone do not provide unambiguous records of temperature and ice volume, hindering assessment of the driving mechanism for these variations. Here we present new benthic foraminiferal Mg/Ca, Li/Ca, and U/Ca records across the Oligocene-Miocene boundary from Ocean Drilling Program Sites 926 and 929. Our records demonstrate that Atlantic bottom-water temperatures varied cyclically, with the main cooling and warming steps followed by ice growth and decay respectively. We suggest that enhanced organic carbon burial acted as a positive feedback as climate cooled. Several lines of evidence suggest that the deglaciation was associated with an input of carbon to the ocean-atmosphere system, culminating in a previously unidentified seafloor dissolution event. We suggest that one of the initial sources of carbon was organic matter oxidation in ocean sediments. This study demonstrates that carbon cycle feedbacks should be considered when evaluating the stability of ancient ice sheets.

INTRODUCTION

The transition from the early Cenozoic greenhouse to the modern icehouse climate has been described as a series of “trends, rhythms, and aberrations” visible in deep-sea benthic oxygen isotope ($\delta^{18}\text{O}$) records (Zachos et al., 2001a, p. 686). In this way, the glaciation event at the Oligocene-Miocene boundary can be thought of as a rhythmic aberration—against a backdrop of moderate ice volume variations paced by Earth’s orbital cycles, the Antarctic ice sheet roughly doubled in size, reaching near-modern proportions for a brief (<400 k.y.) interval termed “Mi-1” (ca. 23 Ma) (Miller et al., 1991; Zachos et al., 2001b; Lear et al., 2004; Liebrand et al., 2011). Although Northern Hemisphere glaciation cannot be ruled out (DeConto et al., 2008), the related sea-level variations (Pekar and DeConto, 2006) reflect at least in part a dynamic East Antarctic Ice Sheet (EAIS), with its advance across the continental shelf correlated to a sea-level fall on the order of 50 m (Naish et al., 2001). This presents a “paleoclimate paradox” given the self-stabilizing (hysteresis) effect in ice sheet models, which results from the difficulty of modeling Antarctic ice melt at high altitude (the ice sheet surface) under realistic boundary conditions (e.g., <900 ppm CO_2 ; Pollard and DeConto, 2005). Concurrent variations in deep-sea $\delta^{13}\text{C}$ records suggest that the carbon cycle may have played a role in the Mi-1 glaciation, perhaps via the biological carbon pump (Zachos et al., 1997; Diester-Haass et al., 2011). However, the dual controls of temperature and ice volume on foraminiferal $\delta^{18}\text{O}$ hinder examination of the temporal relationship between temperature, sea

level, and carbon cycle changes. Mg/Ca paleothermometry is often used to deconvolve the temperature and ice-volume components of $\delta^{18}\text{O}$ records, yet concerns remain regarding a possible saturation state control on benthic foraminiferal Mg/Ca (Elderfield et al., 2006). Here we follow the proposal that infaunal foraminifera living in buffered pore waters may be used as a reliable paleotemperature proxy (Elderfield et al., 2010). We also present a foraminiferal U/Ca record—a promising new proxy for changes in sediment redox state, which is linked to organic carbon burial (Boiteau et al., 2012). We compare our new records with published stable isotope and sediment percent coarse fraction records (Pälike et al., 2006, and references therein), and benthic foraminiferal accumulation rate (BFAR) and total organic carbon (TOC) content records (Diester-Haass et al., 2011). Together, they shed light on the role of the biological carbon pump as a driver of and responder to the climate system, with implications for our understanding of ice sheet dynamics.

MATERIALS AND METHODS

We analyzed the trace metal content (Mg/Ca, Li/Ca, U/Ca, Al/Ca, Mn/Ca, Fe/Ca) of an epifaunal (*Cibicidoides mundulus*) and a shallow infaunal (*Oridorsalis umbonatus*) benthic foraminifera from Ocean Drilling Program (ODP) Site 926 ($3^\circ 43.15' \text{N}$, $42^\circ 54.51' \text{W}$, 3598 m water depth) and Site 929 ($5^\circ 58.57' \text{N}$, $43^\circ 44.40' \text{W}$, 4358 m water depth), drilled on Ceara Rise in the equatorial Atlantic. Today, Site 926 is bathed by North Atlantic Deep Water (NADW), while Site 929 lies within the mixing zone of NADW and Antarctic Bottom Water (Curry et al., 1995). The age model for these sites uses cyclostratigraphy tied to the astronomical solution of Laskar et al. (2004) (Pälike et al., 2006). Benthic foraminifera (150–355 μm) were cleaned using oxidative and reductive steps (Boyle and Keigwin, 1985) and contaminant removal under binocular microscope (Barker et al., 2003). Samples were analyzed at Cardiff University (UK) on a Thermo Element XR inductively coupled plasma–mass spectrometer (ICP-MS) against standards with equivalent Ca concentration. Samples with intensities less than five times the blank were discarded. Analytical precisions determined from consistency standards over the course of one year are 0.5% for Mg/Ca; 4% for Li/Ca and U/Ca; and 2% for Al/Ca, Mn/Ca, and Fe/Ca (rsd, relative standard deviation). Samples with Fe/Mg > 1 mol/mol and/or Al/Ca > 80 $\mu\text{mol/mol}$ were discarded. Fliers within the Mg/Ca and Li/Ca records are provided and plotted in the GSA Data Repository¹ but not plotted in Figure 1. These were identified by being more than two standard deviations offset from the mean of the six bracketing samples in the downcore records. Two species of planktonic foraminifera (*Globigerina praebulloides* [250–300 μm] and *C. dissimilis* [300–355 μm]) were weighed on a six-decimal-place balance to determine average test weight.

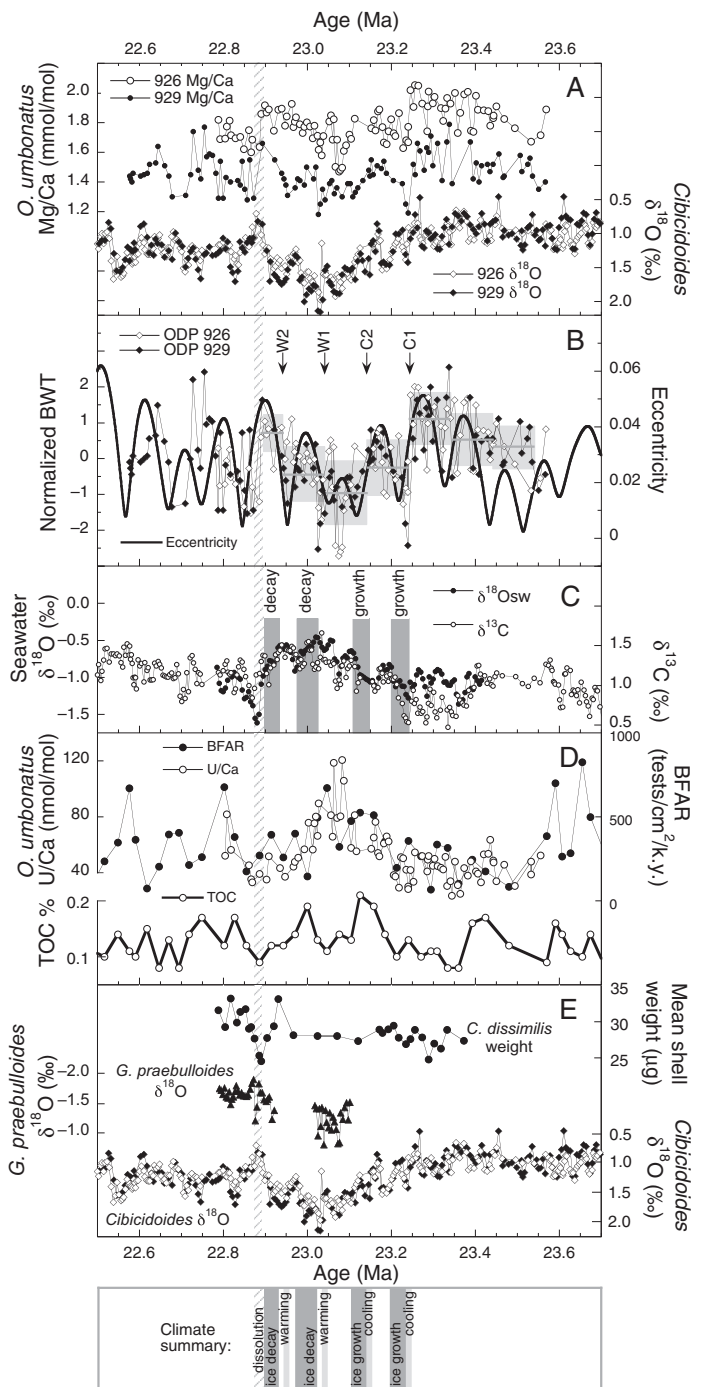
Infaunal Foraminiferal Mg/Ca as a Bottom-Water Temperature Proxy

Benthic foraminiferal Mg/Ca is dominantly controlled by changes in bottom-water temperature (BWT), but an additional saturation state (ΔCO_3^{2-}) control exists below a threshold (Elderfield et al., 2006).

¹GSA Data Repository item 2013270, data tables and Figures DR1–DR3, is available online at www.geosociety.org/pubs/ft2013.htm, or on request from editing@geosociety.org or Documents Secretary, GSA, P.O. Box 9140, Boulder, CO 80301, USA.

*E-mail: learc@cf.ac.uk.

Figure 1. A: *Oridorsalis umbonatus* Mg/Ca (circles) and *Cibicidoides* sp. $\delta^{18}\text{O}$ (diamonds) from Ocean Drilling Program (ODP) Site 926 (open symbols) and Site 929 (closed symbols). $\delta^{18}\text{O}$ data from Pälke et al. (2006, and references therein). **B:** Normalized *O. umbonatus* Mg/Ca bottom-water temperatures (BWT) compared with Earth's eccentricity (Laskar et al., 2004). Normalization was achieved by subtracting the mean and dividing by the standard deviation. Average normalized BWT for seven time slices is shown by horizontal gray bars, with gray boxes representing ± 1 standard deviation. Main cooling and warming steps discussed in text are marked as C1, C2, and W1, W2, respectively. Note that the temperature trend is not correctly captured in highlighted "dissolution event." **C:** Estimated $\delta^{18}\text{O}$ of seawater ($\delta^{18}\text{O}_{\text{sw}}$, solid black circles) and benthic foraminiferal $\delta^{13}\text{C}$ (open circles) from Site 926, with main ice events discussed in text highlighted by gray bars. $\delta^{13}\text{C}$ data from Pälke et al. (2006, and references therein). Note that $\delta^{18}\text{O}_{\text{sw}}$ estimates in highlighted "dissolution event" are biased toward increased deglaciation. **D:** Site 926 *O. umbonatus* U/Ca compared with benthic foraminiferal accumulation rate (BFAR) and percent total organic carbon (TOC) from Diester-Haass et al. (2011). **E:** *Cibicidoides* sp. $\delta^{18}\text{O}$ from Sites 926 and 929 (as in panel A) compared with Site 926 *C. dissimilis* mean test weight (closed circles) and *Globigerina praebulloides* $\delta^{18}\text{O}$ (Pearson et al., 1997). Vertical hatched bar through all panels represents proposed "dissolution event."



Infaunal foraminifera may be protected from ΔCO_3^{2-} changes due to buffering effects, such that Mg/Ca records of a deep infaunal genus, *Uvigerina*, have been interpreted solely in terms of BWT (Elderfield et al., 2010). Here we compare epifaunal and shallow infaunal Mg/Ca records from two water depths, and examine their paired Li/Ca records. We take this approach because although benthic foraminiferal Mg/Ca is positively correlated with temperature and saturation state (Rosenthal et al., 1997; Elderfield et al., 2006), benthic foraminiferal Li/Ca is correlated inversely with temperature (Marriott et al., 2004) and positively with saturation state (Lear and Rosenthal, 2006; Lear et al., 2010). *O. umbonatus* Mg/Ca is 0.33 mmol/mol higher at Site 926 than at Site 929, while *O. umbonatus* Li/Ca is similar at each site (Fig. DR1 in the Data Repository). However, for the epifaunal species *C. mundulus* both mean Mg/Ca and Li/Ca are higher at shallower Site 926 than at Site 929 (by 0.41 mmol/mol and 3.3 $\mu\text{mol/mol}$ respectively). These larger inter-site Mg/Ca and Li/Ca offsets in the epifaunal species point to a greater ΔCO_3^{2-} contrast likely reflecting bottom-water conditions rather than buffered pore waters. If this is the case we note that as today, the water masses bathing ODP Sites 926 and 929 had different $[\text{CO}_3^{2-}]$ during Mi-1. The downcore *C. mundulus* Li/Ca records have larger amplitude variations than the *O. umbonatus* Li/Ca records, also suggesting larger ΔCO_3^{2-} variations (Fig. DR1). In summary, while it is possible that a small saturation-state effect is still present, here *O. umbonatus* Mg/Ca is a more faithful recorder of BWT than *C. mundulus* Mg/Ca. We therefore use the *O. umbonatus* Mg/Ca records with the *O. umbonatus* calibration of Lear et al. (2002) to calculate variations in BWT. We plot normalized BWT in Figure 1 as this does not require estimation of seawater Mg/Ca. However, in the Data Repository we provide BWT calculated assuming both modern and Miocene seawater Mg/Ca (averaging 5 °C and 7 °C respectively at Site 926). Variations in seawater $\delta^{18}\text{O}$ ($\delta^{18}\text{O}_{\text{sw}}$) (Fig. 1C) were calculated using the Site 926 benthic $\delta^{18}\text{O}$ record (Pälke et al., 2006, and references therein) corrected by 0.5‰ (Shackleton and Hall, 1997), with the BWT record assuming modern seawater Mg/Ca and the simplified paleotemperature equation of Shackleton (1974):

$$\delta^{18}\text{O}_{\text{sw}} = \delta^{18}\text{O}_{\text{calcite}} - [(16.9 - \text{BWT})/4.0], \quad (1)$$

where $\delta^{18}\text{O}_{\text{calcite}}$ was corrected to Standard Mean Ocean Water by adding 0.27‰.

Foraminiferal U/Ca as an Indicator of Export Productivity

A recent culture study suggests that seawater carbonate ion concentration affects U speciation in seawater and hence uptake into foraminiferal calcite, such that a 100 $\mu\text{mol/kg}$ decrease in $[\text{CO}_3^{2-}]$ may cause an ~50% increase in foraminiferal U/Ca (Keul et al., 2013). Our U/Ca record increases fourfold between 23.2 Ma and 23.0 Ma, yet our Li/Ca records provide evidence against a major decrease in $[\text{CO}_3^{2-}]$ at this time (Fig. DR2). Instead, our U/Ca increase likely reflects increased authigenic U precipitation under reducing conditions, which is a function of sediment organic carbon content, bottom-water oxygenation levels, and sedimentation rates (Boiteau et al., 2012). The U/Ca increase is associated with the global increase in seawater $\delta^{13}\text{C}$, which may reflect an increased burial ratio of organic to carbonate carbon (Paul et al., 2000), and increased

BFAR (a productivity proxy) (Diester-Haass et al., 2011) (Fig. 1D). The U/Ca increase does not coincide with a change in sedimentation rate (Fig. DR2), which suggests that our U/Ca signal may reflect export productivity (Boiteau et al., 2012).

INSOLATION, CARBON CYCLING, AND CLIMATE

The BWT records display two prominent cooling steps (C1 at ca. 23.24 Ma, and C2 at ca. 23.14 Ma) within the transition into the Mi-1 glacial maximum, and two warming steps (W1 at ca. 23.04, and W2 at ca. 22.94 Ma) within the subsequent recovery phase. The cooling and warming steps are on the order of 1–2 °C and appear to be paced by Earth's short eccentricity cycles (Fig. 1B). The cooling and warming steps are immediately followed by or coincide with intervals of ice growth and decay respectively, as inferred from the calculated $\delta^{18}\text{O}_{\text{sw}}$ record (Fig. 1). One mechanism by which eccentricity modulated variations in Earth's precessional cycles may have impacted BWT is through variations in high-latitude insolation (e.g., a seasonality effect on ice growth; Zachos et al., 2001b). Maximum ice volume is reached at 23.03 Ma following an orbital configuration that led to a relatively long interval of reduced seasonality (Zachos et al., 2001b).

Ice volume and benthic $\delta^{13}\text{C}$ vary in tandem across the record (Fig. 1C). Furthermore, as ice volume increases, so does foraminiferal U/Ca, which we interpret as increased organic carbon burial (Fig. 1D). Mechanistic explanations for the relationship between ice volume and carbon burial include increased meridional temperature gradients leading to greater upwelling and nutrient availability (Zachos et al., 1997; Diester-Haass et al., 2011) and/or a sea level control on nutrient delivery from shelf sediments to the oceans (Liebrand et al., 2011). The foraminiferal $\delta^{13}\text{C}$ reflects a global change in seawater $\delta^{13}\text{C}$ (Paul et al., 2000) while our U/Ca record implies that carbon burial increased specifically at Ceara Rise. Ceara Rise lies in the western equatorial Atlantic and is unlikely to experience significant temporal variations in upwelling (Curry et al., 1995), perhaps favoring a sea-level control on productivity. Regardless, both mechanisms (nutrient delivery from shelves and/or increased upwelling) could potentially lower CO_2 and represent a positive feedback in the climate system.

AN EARLY MIOCENE DEGLACIAL DISSOLUTION EVENT

The final recovery phase of Mi-1 (ca. 22.95 to ca. 22.85 Ma) is marked by a decrease in benthic $\delta^{18}\text{O}$ to pre-excursion values. The majority of this trend is paralleled by a 0.3 mmol/mol increase in *O. umbonatus* Mg/Ca, reflecting ~1.5 °C warming (W2; Fig. 1). However, the last ~20 k.y. of the $\delta^{18}\text{O}$ trend is associated with a decrease in *O. umbonatus* Mg/Ca at both sites (Fig. 1A). The concurrent low values in the Site 926 Li/Ca records argue against a cooling episode (Fig. DR1). This implies that for this brief but significant interval (ca. 22.88 Ma), saturation-state effects dominated over temperature effects on *O. umbonatus* Mg/Ca. Three lines of evidence further suggest this was a seafloor dissolution event:

(1) The percent coarse record from Site 926 (Pälike et al., 2006). Between 23.4 and 22.8 Ma, percent coarse varied cyclically, with an overall trend toward higher values. In general, as observed by other workers, intervals of reduced percent coarse coincide with higher $\delta^{18}\text{O}$, suggesting the influence of a strengthened corrosive bottom-water mass during glacial advances (e.g., Pälike et al., 2006). The one exception to this relationship is at ca. 22.88 Ma, when the percent coarse decreases from >10% to <1% during an interval of decreased $\delta^{18}\text{O}$ (Fig. DR3). Although other controls on percent coarse exist, we interpret this decrease as increased carbonate dissolution.

(2) Published planktonic $\delta^{18}\text{O}$ records (Pearson et al., 1997). Mixed-layer *G. praebulloides* $\delta^{18}\text{O}$ shows an ~0.6‰ excursion to higher values in the middle of the benthic $\delta^{18}\text{O}$ minimum (Fig. 1E). The brief excursion to heavier value(s) at ca. 22.88 Ma is also visible in *P. pseudokugleri* $\delta^{18}\text{O}$, while deep-dwelling *C. dissimilis* $\delta^{18}\text{O}$ displays a tantalizing single sample excursion to low values (Fig. DR3), although further supporting data

are required before this can be interpreted. Dissolution may bias shallow-dwelling planktonic foraminiferal $\delta^{18}\text{O}$ toward higher values, because calcite precipitated in warmer waters is more susceptible to dissolution than calcite precipitated at depth, for example during gametogenesis (Williams et al., 2007).

(3) Planktonic foraminiferal test weight records. The mean test weight of *C. dissimilis* decreases to its lowest value in the proposed dissolution interval (Fig. 1E). We note that *G. praebulloides* mean test weight does not show a similar change, but suggest that their thinner tests were perhaps more susceptible to disintegration having undergone some degree of dissolution than the thicker tests of *C. dissimilis*.

There are several potential mechanisms linking the deglaciation with the proposed dissolution event; we consider just a few here. The first is that the dissolution event at Ceara Rise is a regional signal caused by changes in water mass properties. We do not favor this explanation, but it requires testing using sections at other sites. The second is that rising sea level increased the accommodation space for carbonate platform builders, leading to reduced seawater alkalinity and increased $p\text{CO}_2$ (Opdyke and Walker, 1992). The third possibility we consider is that some of the organic carbon buried in slowly accumulating deep-sea sediments during the glaciation phase of Mi-1 was gradually oxidized, releasing isotopically light carbon to the ocean-atmosphere system. Some support for this is found by comparing our record of foraminiferal U/Ca with the Site 926 percent TOC record (Diester-Haass et al., 2011). Percent TOC increases at 23.2 Ma, as benthic foraminiferal U/Ca increases. At 23.1 Ma, percent TOC decreases while foraminiferal U/Ca continues to increase, hinting at a subsequent burn-down of sedimentary organic carbon (Fig. 1D).

ICE SHEET DYNAMICS

The Oligocene-Miocene glaciation is marked by a transient ~0.6‰ increase in $\delta^{18}\text{O}_{\text{sw}}$, equivalent to a sea-level fall of ~50 m using the Pleistocene calibration of Fairbanks and Matthews (1978). This is in relatively good agreement with estimates using $\delta^{18}\text{O}$ records calibrated to sea level (Pekar and DeConto, 2006), and ~50% higher than estimates derived from inverse modeling (Liebrand et al., 2011). The inverse modeling approach predicts simultaneous bottom-water cooling and ice growth, whereas our records suggest that ice growth immediately followed the main cooling steps. Nevertheless, all approaches imply significant (at least half of the modern Antarctic ice sheet) ice growth and decay across Mi-1. Although Northern Hemisphere glaciation cannot be ruled out, the majority of the ice growth was likely situated in East and West Antarctica (Naish et al., 2001; Bart and De Santis, 2012), with a potentially larger-than-modern ice sheet facilitated by a more favorable paleotopography (Wilson and Luyendyk, 2009). The orbitally paced recovery phase out of the glacial maximum was accompanied by a >2 °C increase in BWT. We propose that this deglaciation phase was associated with a flux of carbon into the ocean-atmosphere system that resulted in a seafloor dissolution event once a saturation-state threshold was crossed. Interestingly, some ice decay preceded the proposed dissolution event. This implies that either (1) carbon cycle perturbations were sufficient to affect the EAIS before the dissolution threshold was reached, (2) ice caps such as the WAIS or Greenland contributed to the deglaciation phase immediately following Mi-1, or (3) ice sheet models may not capture the full dynamic variability of the early Miocene EAIS.

CONCLUSIONS

Orbitally paced variations in bottom-water temperature were associated with ice sheet growth and decay across the Oligocene-Miocene boundary. Glacial conditions favored increased organic carbon burial, which may have acted as a positive feedback as climate cooled. Peak deglacial conditions coincide with a proposed seafloor “dissolution event.” The identification of such carbon cycle perturbations reduces the ice sheet hysteresis problem through CO_2 -induced global warming superimposed on orbital climate variability.

ACKNOWLEDGMENTS

This research used samples provided by the Integrated Ocean Drilling Program (IODP). We thank Jim Zachos for providing some washed samples from Sites 929 and 926. Funding was provided by a NERC grant (NE/1006427/1) to Lear and a NERC studentship (NE/F016603/1) to Mawbey. We thank Stephen Conn for the shell weight analysis, Anabel Morte Rodenas for technical assistance, Liselotte Diester-Haass for sharing published data, and Steve Barker, Hugh Jenkens, Dan Lunt, and Paul Pearson for helpful discussions. This manuscript was improved by the comments of three anonymous reviewers and the editor, Ellen Thomas.

REFERENCES CITED

- Barker, S., Greaves, M., and Elderfield, H., 2003, A study of cleaning procedures used for foraminiferal Mg/Ca paleothermometry: *Geochemistry Geophysics Geosystems*, v. 4, 8407, doi:10.1029/2003GC000559.
- Bart, P.J., and De Santis, L., 2012, Glacial intensification during the Neogene: A review of seismic stratigraphic evidence from the Ross Sea, Antarctica, continental shelf: *Oceanography* (Washington, D.C.), v. 25, p. 166–183, doi:10.5670/oceanog.2012.92.
- Boiteau, R., Greaves, M., and Elderfield, H., 2012, Authigenic uranium in foraminiferal coatings: A proxy for ocean redox chemistry: *Paleoceanography*, v. 27, PA3227, doi:10.1029/2012PA002335.
- Boyle, E.A., and Keigwin, L.D., 1985, Comparison of Atlantic and Pacific paleochemical records for the last 215,000 years: Changes in deep ocean circulation and chemical inventories: *Earth and Planetary Science Letters*, v. 76, p. 135–150, doi:10.1016/0012-821X(85)90154-2.
- Curry, W.B., and Shipboard Scientific Party, 1995, Introduction, in Curry, W.B., et al., eds., *Proceedings of the Ocean Drilling Program, Initial Reports, Volume 154: College Station, Texas, Ocean Drilling Program*, p. 5–10.
- DeConto, R.M., Pollard, D., Wilson, P.A., Palike, H., Lear, C.H., and Pagani, M., 2008, Thresholds for Cenozoic bipolar glaciation: *Nature*, v. 455, p. 652–656, doi:10.1038/nature07337.
- Diester-Haass, L., Billups, K., and Emeis, K., 2011, Enhanced paleoproductivity across the Oligocene/Miocene boundary as evidenced by benthic foraminiferal accumulation rates: *Palaeogeography, Palaeoclimatology, Palaeoecology*, v. 302, p. 464–473, doi:10.1016/j.palaeo.2011.02.006.
- Elderfield, H., Yu, J., Anand, P., Kiefer, T., and Nyland, B., 2006, Calibrations for benthic foraminiferal Mg/Ca paleothermometry and the carbonate ion hypothesis: *Earth and Planetary Science Letters*, v. 250, p. 633–649, doi:10.1016/j.epsl.2006.07.041.
- Elderfield, H., Greaves, M., Barker, S., Hall, I.R., Tripathi, A., Ferretti, P., Crowhurst, S., Booth, L., and Daunt, C., 2010, A record of bottom water temperature and seawater $\delta^{18}\text{O}$ for the Southern Ocean over the past 440 kyr based on Mg/Ca of benthic foraminiferal *Uvigerina* spp.: *Quaternary Science Reviews*, v. 29, p. 160–169, doi:10.1016/j.quascirev.2009.07.013.
- Fairbanks, R.G. and Matthews, R.K., 1978, The oxygen isotope stratigraphy of the Pleistocene reef tracts of Barbados, West Indies: *Quaternary Research*, v. 10, p. 181–196, doi:10.1016/0033-5894(78)90100-X.
- Keul, N., Langer, G., de Noijer, L.J., Nehrke, G., Reichert, G.-J., and Bijma, J., 2013, Incorporation of uranium in benthic foraminiferal calcite reflects seawater carbonate ion concentration: *Geochemistry Geophysics Geosystems*, v. 14, p. 102–111, doi:10.1029/2012GC004330.
- Laskar, J., Robutel, P., Joutel, F., Gastineau, M., Correia, A., and Levrard, B., 2004, A long-term numerical solution for the insolation quantities of the Earth: *Astronomy & Astrophysics*, v. 428, p. 261–285, doi:10.1051/0004-6361:20041335.
- Lear, C.H., and Rosenthal, Y., 2006, Benthic foraminiferal Li/Ca: Insights into Cenozoic seawater carbonate saturation state: *Geology*, v. 34, p. 985–988, doi:10.1130/G22792A.1.
- Lear, C.H., Rosenthal, Y., and Slowey, N., 2002, Benthic foraminiferal Mg/Ca paleothermometry: A revised core-top calibration: *Geochimica et Cosmochimica Acta*, v. 66, p. 3375–3387, doi:10.1016/S0016-7037(02)00941-9.
- Lear, C.H., Rosenthal, Y., Coxall, H.K., and Wilson, P.A., 2004, Late Eocene to early Miocene ice sheet dynamics and the global carbon cycle: *Paleoceanography*, v. 19, PA4015, doi:10.1029/2004PA001039.
- Lear, C.H., Mawbey, E.M., and Rosenthal, Y., 2010, Cenozoic benthic foraminiferal Mg/Ca and Li/Ca records: Toward unlocking temperatures and saturation states: *Paleoceanography*, v. 25, PA4215, doi:10.1029/2009PA001880.
- Liebrand, D., Lourens, L.J., Hodell, D.A., de Boer, B., van de Wal, R.S.W., and Pälike, H., 2011, Antarctic ice sheet and oceanographic response to eccentricity forcing during the early Miocene: *Climate of the Past*, v. 7, p. 869–880, doi:10.5194/cp-7-869-2011.
- Marriott, C.S., Henderson, G.M., Crompton, R., Staubwasser, M., and Shaw, S., 2004, Effect of mineralogy, salinity, and temperature on Li/Ca and Li isotope composition of calcium carbonate: *Chemical Geology*, v. 212, p. 5–15, doi:10.1016/j.chemgeo.2004.08.002.
- Miller, K.G., Wright, J.D., and Fairbanks, R.G., 1991, Unlocking the ice house: Oligocene-Miocene oxygen isotopes, eustasy, and margin erosion: *Journal of Geophysical Research*, v. 96, p. 6829–6848, doi:10.1029/90JB02015.
- Naish, T.R., and 32 others, 2001, Orbitally induced oscillations in the East Antarctic ice sheet at the Oligocene/Miocene boundary: *Nature*, v. 413, p. 719–723, doi:10.1038/35099534.
- Opdyke, B.N., and Walker, J.C.G., 1992, Return of the coral reef hypothesis: Basin to shelf partitioning of CaCO_3 and its effect on atmospheric CO_2 : *Geology*, v. 20, p. 733–736, doi:10.1130/0091-7613(1992)020<0733:ROTCRH>2.3.CO;2.
- Pälike, H., Frazier, J., and Zachos, J., 2006, Extended orbitally forced palaeoclimatic records from the equatorial Atlantic Ceara Rise: *Quaternary Science Reviews*, v. 25, p. 3138–3149, doi:10.1016/j.quascirev.2006.02.011.
- Paul, H., Zachos, J., Flower, B., and Tripathi, A., 2000, Orbitally induced climate and geochemical variability across the Oligocene/Miocene boundary: *Paleoceanography*, v. 15, p. 471–485, doi:10.1029/1999PA000443.
- Pearson, P.N., Shackleton, N.J., Weedon, G.P., and Hall, M.A., 1997, Multi-species planktonic foraminifer stable isotope stratigraphy through Oligocene/Miocene boundary climatic cycles, Site 926, in Shackleton, N.J., et al., eds., *Proceedings of the Ocean Drilling Program, Scientific Results, Volume 154: College Station, Texas, Ocean Drilling Program*, p. 441–449.
- Pekar, S.F., and DeConto, R.M., 2006, High-resolution ice-volume estimates for the early Miocene: Evidence for a dynamic ice sheet in Antarctica: *Palaeogeography, Palaeoclimatology, Palaeoecology*, v. 231, p. 101–109, doi:10.1016/j.palaeo.2005.07.027.
- Pollard, D., and DeConto, R.M., 2005, Hysteresis in Cenozoic Antarctic ice-sheet variations: *Global and Planetary Change*, v. 45, p. 9–21, doi:10.1016/j.gloplacha.2004.09.011.
- Rosenthal, Y., Boyle, E.A., and Slowey, N., 1997, Temperature control on the incorporation of magnesium, strontium, fluorine, and cadmium into benthic foraminiferal shells from Little Bahama Bank: Prospects for thermocline paleoceanography: *Geochimica et Cosmochimica Acta*, v. 61, p. 3633–3643, doi:10.1016/S0016-7037(97)00181-6.
- Shackleton, N.J., 1974, Attainment of isotopic equilibrium between ocean water and benthonic foraminifera genus *Uvigerina*: Isotopic changes in the ocean during the last glacial, in *Les Méthodes Quantitatives D'étude des Variations du Climat au Cours du Pleistocène: Gif-sur-Yvette, France, Le Centre National de la Recherche Scientifique*, p. 203–209.
- Shackleton, N.J., and Hall, M.A., 1997, The late Miocene stable isotope record, Site 926, in Shackleton, N.J., et al., eds., *Proceedings of the Ocean Drilling Program, Scientific Results, Volume 154: College Station, Texas, Ocean Drilling Program*, p. 367–373.
- Williams, M., Haywood, A.M., Vautravers, M., Sellwood, B.W., Hillenbrand, C.-D., Wilkinson, I.P., and Miller, C.G., 2007, Relative effect of taphonomy on calcification temperature estimates from fossil planktonic foraminifera: *Geobios*, v. 40, p. 861–874, doi:10.1016/j.geobios.2007.02.007.
- Wilson, D.S., and Luyendyk, B.P., 2009, West Antarctic paleotopography estimated at the Eocene-Oligocene transition: *Geophysical Research Letters*, v. 36, L16302, doi:10.1029/2009GL039297.
- Zachos, J.C., Flower, B.P., and Paul, H., 1997, Orbitally paced climate oscillations across the Oligocene/Miocene boundary: *Nature*, v. 388, p. 567–570, doi:10.1038/41528.
- Zachos, J., Pagani, M., Sloan, L., Thomas, E., and Billups, K., 2001a, Trends, rhythms, and aberrations in global climate 65 Ma to present: *Science*, v. 292, p. 686–693, doi:10.1126/science.1059412.
- Zachos, J.C., Shackleton, N.J., Revenaugh, J.S., Pälike, H., and Flower, B.P., 2001b, Climate response to orbital forcing across the Oligocene-Miocene boundary: *Science*, v. 292, p. 274–278, doi:10.1126/science.1058288.

Manuscript received 25 January 2013

Revised manuscript received 17 April 2013

Manuscript accepted 18 April 2013

Printed in USA